Doppler effects of inertial currents on subsurface temperature measurements

by T. H. Bell, Jr.[1]

ABSTRACT

In the presence of inertial oscillations, temperature measurements from a moored sensor will be contaminated by advected spatial structure. The degree of contamination is comparable to that induced by steady currents of the same magnitude, and its effect resembles that of a discrete linear filter acting on the spectrum, with filter response contributions at the sum and difference frequencies $\omega \pm nf$, where ω is the sample frequency and f the inertial frequency. Strong inertial currents may induce spectral peaks at harmonics of the inertial frequency. If the spectrum includes discrete components such as the internal tide, secondary peaks will be induced at the sum and difference frequencies $\omega_0 \pm nf$, where ω_0 is the frequency of the discrete component.

1. Introduction

The oceanic temperature field is a random function of space and time. In recent years, a considerable amount of work has been devoted to the problem of modeling the statistical properties of this random field. Of particular interest are problems relating to the interpretation of data from moored temperature sensors in the range of frequencies characteristic of internal wave motions (that is, between the local inertial frequency and the Brunt-Väisälä frequency, see Garrett and Munk, 1972). A number of authors (Phillips, 1971, and Garrett and Munk, 1971, among others) have considered the problem of contamination of data from moored temperature sensors by the kinematic interaction of internal waves and vertical microstructure. Others (White, 1972, and Garrett and Munk, 1972, for example) have considered the Doppler smearing of internal wave spectra by steady currents. Here, we consider the Doppler effect of inertial oscillations on data from moored temperature sensors.

Pure inertial oscillations involve only horizontal motions, and as such do not contribute directly to the temperature variability, which is generally related to vertical motions. However, inertial currents will advect the random temperature field past a moored sensor, so that the temperature variability seen by the sensor will not reflect the true temporal structure of the random field, but will in fact be contami-

1. Ocean Sciences Division, Naval Research Laboratory, Washington, D.C., 20375, U.S.A.

nated by advected spatial structure. The effect of this contamination on the frequency spectrum is shown to resemble that of a discrete linear filter, whose response includes contributions from the sums and differences of the sample frequency and the inertial frequency and its harmonics. The relative weights of the contributions are determined by the horizontal coherence of the temperature field. The distortion of a representative model spectrum (Garrett and Munk, 1972, 1975) has been calculated for several magnitudes of the inertial frequency current, and is found to be comparable to that induced by steady currents of the same magnitude. Strong inertial frequency currents (> 20 cm/sec) may induce sensible peaks (> 1 dB above the continuum) in the spectrum at harmonics of the inertial frequency. The effect of inertial oscillations on discrete spectral components such as the internal tide is also considered. The inertial frequency currents are found to induce secondary spectral peaks at the sum and difference frequencies $\omega_0 \pm nf$, where ω_0 and f are the tidal and inertial frequencies. For strong inertial currents (> 20 cm/sec), more than 50% of the tidal energy may be transferred to these sidebands.

2. General Theory

The temperature field $T(\mathbf{x},t)$ is assumed to be a stationary, homogeneous random function of space and time. If this random field is advected past a moored sensor at a velocity $\mathbf{U}(t)$, then the time series of temperature sampled at the sensor, $\hat{T}(t)$, is given by

$$\hat{T}(t) = T[\mathbf{x}(t),t] \tag{2.1}$$

where

$$\mathbf{x}(t) = -\int_0^t \mathbf{U}(t)\, dt \ . \tag{2.2}$$

The sample correlation function is then given by

$$\begin{aligned} \hat{R}(t) &= < \hat{T}(o)\ \hat{T}(t) > \\ &= R[\mathbf{x}(t),\ t] \end{aligned} \tag{2.3}$$

where $R(x,t) = < T(0,0)\ T(x,t) >$ is the space-time correlation function of the homogeneous random field T, angular brackets being used to denote probability averages. The sample power spectrum is related to the Fourier transform

$$\hat{F}(\omega) = \int_{-\infty}^{\infty} \hat{R}(t) e^{-i\omega t} dt \tag{2.4}$$

with inverse

$$\hat{R}(t) = \frac{1}{2\pi} \int_{-\infty}^{\infty} \hat{F}(\omega) e^{i\omega t} d\omega \ . \tag{2.5}$$

As normally plotted, the power spectrum would be given by $2\hat{F}(\omega/2\pi)$ where

$\omega/2\pi$ is circular frequency (cycles per unit time) and the temperature variance $< T^2 >$ is equal to the integral of the spectrum over all positive circular frequencies. In the sequel, however, we will simply refer to $\hat{F}(\omega)$ as the sample power spectrum. Substituting from equation (2.3) into (2.4), then

$$\hat{F}(\omega) = \int_{-\infty}^{\infty} R[\mathbf{x}(t),t]e^{-i\omega t}dt \ . \tag{2.6}$$

The correlation function $R(\mathbf{x},t)$ may be expressed as

$$R(\mathbf{x},t) = \frac{1}{2\pi}\int_{-\infty}^{\infty} F(\omega)\ C(\mathbf{x},\omega)e^{i\omega t}d\omega \tag{2.7}$$

where $F(\omega)$ is the true power spectrum of the random temperature field which would be obtained in the absence of advection currents

$$F(\omega) = \int_{-\infty}^{\infty} R(o,t)e^{-i\omega t}dt \tag{2.8}$$

and $C(\mathbf{x},\omega)$ is the moored horizontal coherence

$$C(\mathbf{x},\omega) = \frac{\int_{-\infty}^{\infty} R(\mathbf{x},t)e^{-i\omega t}dt}{\int_{-\infty}^{\infty} R(o,t)e^{-i\omega t}dt} \ . \tag{2.9}$$

Substituting from equation (2.7) into (2.6), then

$$\hat{F}(\omega) = \int_{-\infty}^{\infty} F(\omega')W(\omega,\omega')\,d\omega' \tag{2.10}$$

where

$$W(\omega,\omega') = \frac{1}{2\pi}\int_{-\infty}^{\infty} C[\mathbf{x}(t),\omega']e^{i(\omega'-\omega)t}dt \ . \tag{2.11}$$

Equation (2.10) illustrates that the Doppler effect of any advective current may be modeled by a linear filter acting on the power spectrum. The impulse response of the filter is given by equation (2.11).

The relationship between the filter response and the spatial coherence of the temperature field is best illustrated by considering the case of a steady current. In this case, x is directly proportional to time, t, and equation (2.11) takes the form of a Fourier transform. Recalling the fundamental properties of Fourier transform pairs, it is clear that the "peakedness" of the filter response or the degree of spectral smoothing is related to the "peakedness" of the coherence function and the magnitude of the current. This relationship is illustrated in Fig. 1. A highly peaked coherence function results in a broad filter response and a high degree of spectral smoothing, while a broad coherence function results in a peaked filter response and

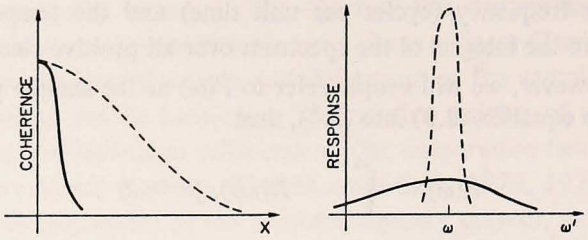

Figure 1. The inverse relationship between horizontal coherence of the temperature field and the response of the spectral smoothing filter for Doppler smearing by steady currents.

less smoothing. This is a manifestation of the fact that the spectral contamination is due to the advection of incoherent spatial structure. If there were no spatial structure in the temperature field, that is, if it were spatially coherent, then there would be no contamination, whereas if the spatial structure were completely incoherent, the sample spectrum would be white. Since the magnitude of the current determines the scaling of distance, an increase in current speed results in an apparent increase in the peakedness of the coherence function, and hence an increase in the degree of smoothing.

The situation is somewhat more complicated when inertial frequency currents are considered. In this case, the temperature field is sampled along a trajectory $\mathbf{x}(t)$ with components

$$\begin{aligned} x_1(t) &= (2U/f)\sin(ft/2)\cos(ft/2+\phi) \\ x_2(t) &= (2U/f)\sin(ft/2)\sin(ft/2+\phi) \end{aligned} \tag{2.12}$$

where $\mathbf{x} = (x_1,x_2)$, f is the inertial frequency, U is the magnitude of the inertial current, and ϕ is an arbitrary phase angle. Since the temperature field is statistically homogeneous, the coherence depends only on the magnitude of $\mathbf{x}$:

$$x(t) = \frac{2U}{f}\left|\sin\left(\frac{ft}{2}\right)\right| . \tag{2.13}$$

Since $x(t)$ is periodic, $C[x(t), \omega']$ is periodic in time, and the integral in equation (2.11) does not exist in the normal sense. We may proceed formally, however, by expanding the coherence function in a Fourier series:

$$C[x(t),\omega'] = \sum_{n=-\infty}^{\infty} a_n(\omega')e^{inft} \tag{2.14}$$

where

$$a_n(\omega') = \frac{f}{2\pi}\int_{-\pi/f}^{\pi/f} C[x(t),\omega']e^{-inft}dt . \tag{2.15}$$

The weight function or filter response $W(\omega,\omega')$ is then given as a series of δ-functions:

$$W(\omega,\omega') = \sum_{n=-\infty}^{\infty} a_n(\omega')\,\delta(\omega' - \omega = nf) \quad . \tag{2.16}$$

The sample spectrum is then given by

$$\hat{F}(\omega) = \sum_{n=-\infty}^{\infty} a_n(\omega - nf)\,F(\omega - nf) \quad , \tag{2.17}$$

which describes the effect of a discrete linear filter. The sample spectrum $\hat{F}(\omega)$ is thus obtained by superimposing weighted, frequency shifted images of the spectrum $F(\omega)$ onto itself. The frequency shifts are in integral multiples of the inertial frequency, and the weights are frequency dependent. At a particular sample frequency ω, the sample spectrum $\hat{F}(\omega)$ is a weighted sum of contributions from the true spectrum at the sample frequency and all of the sum and difference frequencies $\omega \pm nf$.

3. Continuous spectra

The moored horizontal coherence $C(x,\omega)$ of the temperature field has been estimated by Briscoe (1975) for horizontal lags x ranging from 14 m to 1600 m using 40 days of continuous data from the IWEX array in the western North Atlantic. For frequencies less than the local Brunt-Väisälä frequency, the coherence function appears to depend on the product ωx rather than on ω and x independently. Briscoe has examined the results of eight other experiments summarized by Siedler (1974) as well as some of the IWEX results, and concludes that the "half-coherence frequency" $\omega_{1/2}$, where $C(x,\omega_{1/2}) = 1/2$, may be represented by

$$\omega_{1/2} = 1/\alpha x \tag{3.1}$$

where $\alpha = 0.58$ m/sec. The IWEX data is replotted in Fig. 2 as a function of ωx. Also shown in Fig. 2 is a simple curve of the form

$$C(x,\omega) = \frac{1}{1 + (\alpha\omega x)^2} \tag{3.2}$$

which appears to describe the data adequately, and which may be used in estimating Doppler effects on internal wave spectra using the theory developed in the preceding section. Although it is probable that the coherence estimates are also contaminated by Doppler effects, we expect that, since the Doppler effects are generally small, the representation (3.2) will be sufficiently accurate for estimating Doppler effects on internal wave spectra.

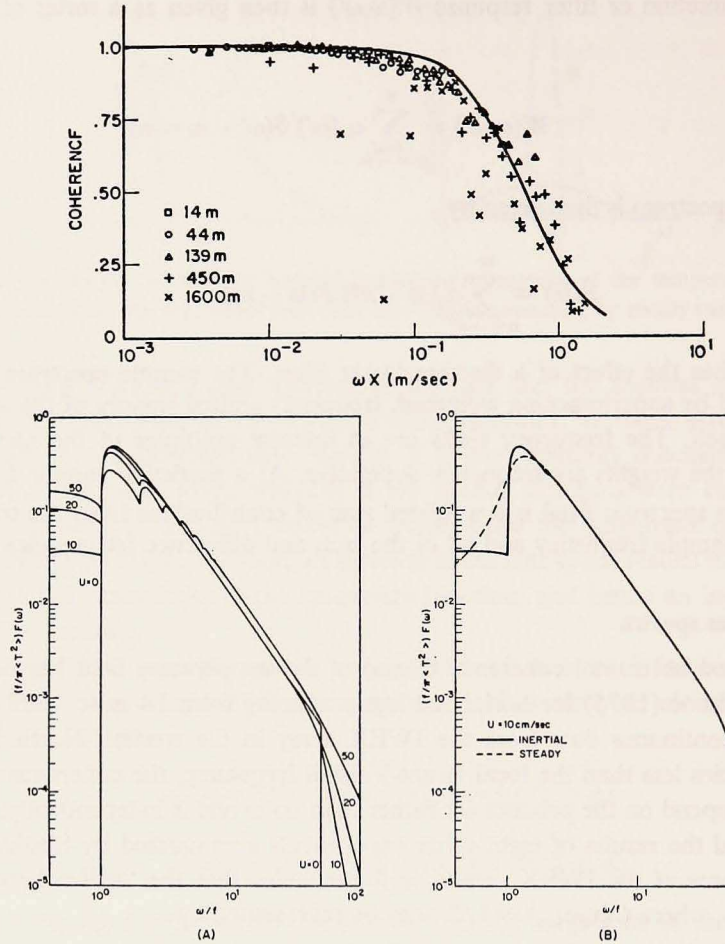

Figure 2. Moored horizontal coherence of temperature from the IWEX data (after Briscoe, 1975). Curve is the model given by equation (3.2).

Figure 3A. Normalized internal wave spectra in the presence of inertial currents of magnitude U (cm/sec). 3B. Comparison of normalized internal wave spectra in the presence of inertial and steady currents of magnitude 10 cm/sec.

Substituting from equation (2.13) for $x(t)$ in the case of an inertial current of magnitude U into equation (3.2), we have

$$C[x(t),\omega] = \{1 + 4\alpha^2\omega^2L^2 \sin^2 (ft/2)\}^{-1}$$
$$= \{1 + 2\alpha^2\omega^2L^2 [1 - \cos (ft)]\}^{-1} \tag{3.3}$$

where $L = U/f$ is the radius of the horizontal orbital motion of the inertial oscilla-

tion, and may be of order 1 km (Phillips, 1966, § 5.7). The Fourier series representation of equation (3.3) is readily obtained by setting

$$1 + \frac{1}{2\alpha^2\omega^2 L^2} = \cosh(\xi) \tag{3.4}$$

and

$$e^{-\xi} = r \ . \tag{3.5}$$

Equation (3.3) then becomes

$$\begin{aligned} C[x(t),\omega] &= \tanh(\xi/2)\,\frac{\sinh(\xi)}{\cosh(\xi) - \cos(ft)} \\ &= \frac{1-r}{1+r}\quad\frac{1-r^2}{1-2r\cos(ft)+r^2} \end{aligned} \tag{3.6}$$

which is a well known form arising in the study of Laplace's equation in a circular region. The Fourier series representation is given by Carslaw (1950, §99):

$$\begin{aligned} C[x(t),\omega] &= \frac{1-r}{1+r}\left\{\ 1 + 2\ \sum_{n=1}^{\infty} r^n \cos(nft)\ \right\} \\ &= \tanh(\xi/2)\left\{\ 1 + 2\ \sum_{n=1}^{\infty} e^{-n\xi}\cos(nft)\right\} \end{aligned} \tag{3.7}$$

From equations (2.17) and (2.14), then, the sample spectrum $\hat{F}(\omega)$ is given by

$$\hat{F}(\omega) = \sum_{n=-\infty}^{\infty} e^{-|n|\zeta_n} \tanh(\zeta_n/2)\, F(\omega_n) \tag{3.8}$$

where $F(\omega)$ is the uncontaminated spectrum, $\omega_n = \omega - nf$, and ζ_n is defined by equation (3.4) with ω_n and ζ_n replacing ω and ζ. Note that

$$\begin{aligned} \tanh^2(\zeta_n/2) &= \frac{1}{1 + 4\alpha^2 U^2 \omega_n^2/f^2} \\ e^{-\zeta_n} &= \frac{1 - \tanh(\zeta_n/2)}{1 + \tanh(\zeta_n/2)} \end{aligned} \tag{3.9}$$

which illustrates that the filter response in equation (3.8) could be expressed directly in terms of the coherence $C(2L,\omega)$.

To illustrate the Doppler effect, we apply equation (3.8) to a model internal wave spectrum

$$\begin{aligned} F(\omega) &= \frac{4\, f^2 < T^2 > (\omega^2 - f^2)^{\frac{1}{2}}}{|\omega|^3}\ , \ f^2 < \omega^2 < N^2 \\ &= 0, \text{ otherwise} \end{aligned} \tag{3.10}$$

where N is the Brunt-Väisälä frequency and $< T^2 >$ is the temperature variance assuming $N^2 >> f^2$ (see Garrett and Munk, 1972, 1975). The results are shown in

Fig. 3a for several values of the magnitude of the inertial current, with $N = 50f$. Clearly, if the inertial currents are sufficiently strong ($U \geqq 20$ cm/sec), significant structure may be introduced into an otherwise smooth spectrum. It is of interest to compare these results with the results of similar calculations of Doppler contamination by steady currents. In the case of a steady current of speed U

$$C[x(t),\omega] = \frac{1}{1 + \alpha^2\omega^2U^2t^2} \cdot \tag{3.11}$$

The Fourier transform of this expression is well known (see Carslaw, 1950, p. 322), so that by equations (2.11) and (2.10),

$$\hat{F}(\omega) = \frac{1}{2\alpha U}\int_{-\infty}^{\infty} \frac{F(\omega')}{|\omega|'} \exp[-|1-\omega/\omega'|/\alpha U]\, d\omega' \cdot \tag{3.12}$$

The sample spectrum for a steady current of 10 cm/sec with $F(\omega)$ given by equation (3.10) is compared with that for an inertial current of the same magnitude in Fig. 3b. Although somewhat different in form, the Doppler effects for steady and inertial currents are comparable in magnitude. The difference is restricted to relatively low frequencies, as is to be expected since the steady flow solution (3.12) may be obtained from the inertial current solution (3.8) in the limit $\omega/f \to \infty$.

4. Discrete spectra

We now consider the Doppler effect of inertial currents on discrete spectral components such as the internal tide. Consider first the effect on a coherent wave of the form

$$T(\mathbf{x},t) = T_0 \cos(\mathbf{k}\cdot\mathbf{x} - \omega_0 t) \tag{4.1}$$

where $\mathbf{k} = (k_1,k_2)$ is the wavenumber and ω_0 the frequency of the coherent wave. The sampled time series of temperature is

$$\begin{aligned} \hat{T}(t) &= T[\mathbf{x}(t),t] \\ &= T_0 \cos[\mathbf{k}\cdot\mathbf{x}(t) - \omega_0 t] \end{aligned} \tag{4.2}$$

where $\mathbf{x}(t)$ is the sample trajectory. With $x(t)$ given by equation (2.12), we have

$$\hat{T}(t) = T_0 \cos[kL \sin(ft - \theta) - \omega_0 t + u] \tag{4.3}$$

where θ is an arbitrary phase, $u = kL \sin\theta$, k is the wavenumber magnitude, and as before, $L = U/f$ is the radius of the horizontal orbital motion of the inertial oscillation. The expression (4.3) may be expanded in a series of simple harmonic functions of time by invoking the fundamental expansion for Bessel functions in the form

$$e^{iz\sin(\beta)} = \sum_{n=-\infty}^{\infty} e^{in\beta} J_n(z) \tag{4.4}$$

(see Watson, 1966, §§ 2.1, 2.22), so that

$$\hat{T}(t) = T_0 \sum_{n=-\infty}^{\infty} J_n(kL) \cos [(\omega_0 - nf)\, t + \phi_n] \tag{4.5}$$

with $\phi_n = kL \sin(\theta) - n\theta$, θ being an arbitrary phase angle as noted previously. Thus, the sampled time series contains an entire discrete spectrum of oscillations at the sum and difference frequencies $\omega_0 \pm nf$. The amplitude at frequency ω_0 is reduced to $T_0\, J_0\, (kL)$, while the sideband amplitudes are given by $T_0\, J_n\, (kL)$. If we consider a first mode internal tide with $k \approx 0.05\ km^{-1}$ (Krupin, 1969), then for $L \approx 1$ km we have $kL << 1$ and may approximate

$$J_n(kL) \approx \frac{1}{n!} (\tfrac{1}{2}kL)^n \tag{4.6}$$

for $n \geqq 0$, with $J_n(kL) = (-1)^n\, J_n(kL)$. The amplitudes of the first sidebands ($\omega_0 \pm f$) are then only a few percent of the primary frequency amplitude, and those of higher order sidebands are proportionately smaller. For the sidebands to be of comparable amplitude to the primary oscillation, kL must be of order unity, or $L \approx 20$ km, corresponding to an inertial current of roughly 1.5 m/sec. Thus, inertial oscillations may in general be expected to have a negligible effect on observations of coherent first-mode internal tides. The situation may be somewhat different when the internal tide is composed of an entire spectrum of wavelengths, such as might occur if a generation mechanism such as that described by Bell (1973, 1975) were operative.

The discrete spectrum corresponding to the sample time series of equation (4.5) is given by

$$\hat{F}(\omega) = 2\pi\, T_0{}^2 \sum_{n=-\infty}^{\infty} J_n{}^2(kL)\, \delta(\omega - \omega_0 + nf)\ . \tag{4.7}$$

If an entire spectrum of wavelengths is present, then equation (4.7) must be averaged over wavenumber. The appropriate probability density function is $(2\pi T_0)^{-1}$ times the wavenumber spectrum $F(\mathbf{k})$, since the spectrum describes the distribution of variance over wavenumber space, with

$$T_0{}^2 = \frac{1}{4\pi^2} \int_{-\infty}^{\infty} F(\mathbf{k}) d\mathbf{k} \tag{4.8}$$

and

$$F(\mathbf{k}) = \int_{-\infty}^{\infty} R_0(\mathbf{x}) e^{-i\mathbf{k}\cdot\mathbf{x}} d\mathbf{x} \tag{4.9}$$

in which $R_0(\mathbf{x})$ is the spatial correlation function for waves of frequency ω_0. Averaging over wavenumber, then, we have

$$\hat{F}(\omega) = \sum_{n=-\infty}^{\infty} \int_0^{\infty} kJ_n^2(kL)\, F(k)dk\, \delta(\omega - \omega_0 + nf) \tag{4.10}$$

assuming an isotropic spectrum, that is, that $F(\mathbf{k})$ depends only on the magnitude of $\mathbf{k}$. Invoking the integral representation

$$J_n^2(kL) = \frac{1}{\pi} \int_0^{\pi} J_0[2kL \sin(\beta)] \cos(2n\beta)\, d\beta \tag{4.11}$$

(Watson, 1966, § 2.6), the integral in equation (4.11) may be transformed to

$$\int_0^{2\pi} \left\{ \frac{1}{2\pi} \int_0^{\infty} kJ_0[2kL \sin(\beta/2)]\, F(k)\, dk \right\} \cos(n\beta)\, d\beta \ . \tag{4.12}$$

The inner integral in expression (4.12) is easily identified as the inverse of equation (4.9) for an isotropic spectrum, with $x = 2L \sin(\beta/2)$, so that equation (4.10) becomes

$$\hat{F}(\omega) = \sum_{n=-\infty}^{\infty} \int_0^{2\pi} R_0[2L \sin(\beta/2)] \cos(n\beta)\, d\beta\, \delta(\omega - \omega_0 + nf) \tag{4.13}$$

The correlation $R_0(x)$ is formally equivalent to T_0^2 times the coherence at frequency ω_0, so that we may express

$$\hat{F}(\omega) = 2\pi\, T_0^2 \sum_{n=-\infty}^{\infty} a_n \delta(\omega - \omega_0 + nf) \tag{4.14}$$

where

$$a_n = \frac{1}{2\pi} \int_0^{2\pi} C[2L \sin(\beta/2), \omega_0] \cos(n\beta)\, d\beta \ . \tag{4.15}$$

This expression for the discrete sample spectrum is precisely that which would be obtained by applying the general theory developed in § 2 above to a discrete spectrum of the form $F(\omega) = 2\pi\, T_0^2 \delta(\omega - \omega_0)$.

Barnett and Bernstein (1975) have measured the horizontal coherence of semidiurnal internal tides in the central Pacific over distances ranging from 5 km to 500 km. They find a coherence of 0.7 at 5 km, and no significant coherence at 50 km or 500 km. These results are consistent with the IWEX data plotted in Fig. 2, which also contains contributions from internal tides. If the coherence function given by equation (3.2) is then taken to be representative of mid-ocean internal tides, the analysis of the preceding section is applicable, and the coefficients a_n in equation (4.14) above are given by

$$a_n = \tanh(\zeta/2)\, e^{-|n|\zeta} \tag{4.16}$$

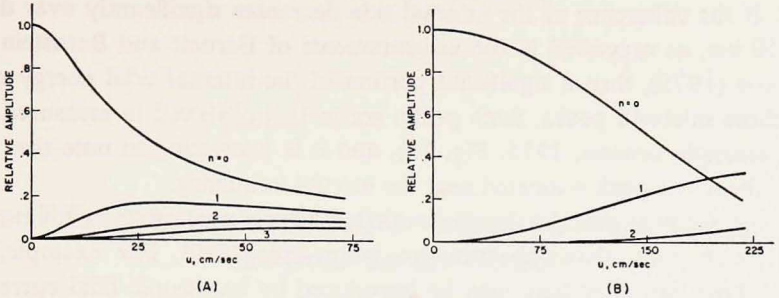

Figure 4A. Relative amplitudes of spectral peaks at frequencies $\omega_0 \pm nf$ as a function of the magnitude of the inertial current, where ω_0 is the frequency of the internal tide, assuming a coherence function given by equation (3.2). 4B. Same as A, assuming a coherent first mode internal tide.

where

$$\cosh(\zeta) = 1 + \frac{1}{2\alpha^2\omega_0^2 L^2}$$

with $\alpha^{-1} \sim 0.58$ m/sec. The a_n are the relative amplitudes of the peaks in the sample spectrum. In the absence of inertial currents ($U = 0$), $a_0 = 1$ and $a_n = 0$ for $n \neq 0$. Values of the coefficients for several values of n are plotted as a function of U in Fig. 4a, assuming $\omega_0 \approx 2f$, which is appropriate for the semidiurnal tide at mid latitudes. For weak inertial currents ($U \leqq 5$ cm/sec) the primary spectral peak at ω_0 dominates, with less than 5% of the energy appearing in the secondary peaks. For strong inertial currents ($U \geqq 25$ cm/sec), however, less than half the energy remains in the primary peak, and the secondary peaks become significant. A similar plot of a_n as a function of U for a single coherent first-mode internal tide is shown in Fig. 4b. Here a_n is given by equation (4.7) as $J_n^2(kL)$. Clearly, if the internal tide is characterized by a single coherent wave rather than a spectrum of waves of varying length, then the Doppler effects of inertial currents are significantly reduced.

5. Conclusion

We have investigated the Doppler effect of inertial currents on temperature measurements from moored sensors. For moderate inertial currents (of order 10 cm/sec or less), the primary effect on the internal wave spectrum is the appearance of energy at sub-inertial frequencies and frequencies above the buoyancy cut-off. Strong inertial currents ($\geqq 20$ cm/sec) may induce significant structure in the measured spectrum, in the form of sensible peaks near harmonics of the inertial frequency. If the internal wave field contains a discrete harmonic component at frequency ω_0, such as an internal tide, then the sample spectrum will display peaks not only at the primary frequency but also at the sum and difference frequencies

$\omega_0 \pm nf$. If the coherence of the internal tide decreases significantly over distances of 5 or 10 km, as suggested in the measurements of Barnett and Bernstein (1975) and Briscoe (1975), then a significant portion of the internal tidal energy may appear in these sideband peaks. Such peaks are in fact observed in measured spectra (see, for example Briscoe, 1975, Fig. 15), and it is interesting to note that at mid-latitudes, the $n = 1$ peak is located near the inertial frequency.

In closing, we note that the theory developed here is applicable to any oscillatory currents which may advect the random temperature field. For example, effects similar to those described here may be introduced by barotropic tidal currents (see Bell, 1973).

REFERENCES

Barnett, T. P., and R. L. Bernstein. 1975. Horizontal scales of midocean internal tides. J. Geophys. Res., *80*, 1962–1964.

Bell, T. H. 1973. Internal wave generation by deep ocean flows over abyssal topography. PhD. thesis, The Johns Hopkins University, Baltimore, 130 pp.

—— 1975. Topographically generated internal waves in the open ocean. J. Geophys. Res., *80*, 320–327.

Briscoe, M. G. 1975. Preliminary results from the trimoored internal wave experiment (IWEX). J. Geophys. Res., *80*, 3872–3884.

Carslaw, H. S. 1950. Introduction to the theory of Fourier's series and integrals. New York, Dover, 368 pp.

Garrett, C. and W. Munk. 1971. Internal wave spectra in the presence of fine-structure. J. Phys. Ocean., *1*, 196–202.

—— 1972. Space-time scales of internal waves. Geophys. Fluid Dyn., *3*, 225–264.

—— 1975. Space-time scales of internal waves: a progress report. J. Geophys. Res., *80*, 291–297.

Krupin, V. D. 1969. A property of internal waves. Soviet Physics, Acoustics, *15*, 69–74.

Phillips, O. M. 1966. The dynamics of the upper ocean. London, Cambridge Univ. Press, 261 pp.

—— 1971. On spectra measured in an undulating layered medium. J. Phys. Ocean., *1*, 1–6.

Siedler, G. 1974. Observations of internal wave coherence in the deep ocean. Deep-Sea Res., *21*, 597–610.

Watson, G. N. 1966. A treatise on the theory of Bessel functions. London, Cambridge Univ. Press, 804 pp.

White, W. B. 1972. Doppler shift in the frequency of inertial waves observed in moored spectra. Deep-Sea Res., *19*, 595–600.

Received: *23 January, 1976;* revised: *12 May, 1976.*